Investigating the dual role of geocells in slope stabilization: Reinforcement and fascia

Sureka S[1], and Arindam Dey[1]

[1] Department of Civil Engineering, IIT Guwahati, Guwahati, 781039, India.

ABSTRACT

Geocells, among other types of geosynthetics, gets its limelight due to the confinement effect that can be provided by its three-dimensional honeycomb structure. Soil infilled geocell pockets stacked one above the other forms a retaining system just by its self-weight. In this study, geocell layers are introduced as reinforcements in slopes and its behaviour under seismic loading is investigated in comparison with the behaviour of geocells as fascia. In this regard, 1g shake table tests have been conducted on lab-scale models constructed with geocells introduced as fascia and reinforcements under seismic loading. The seismic responses in terms of acceleration, displacement of the slope face, lateral stress exerted by the backfill and the corresponding tensile strains developed in geocell walls are studied in response to two different seismic magnitudes. Hysteresis behaviour of the lab-scale models is numerically investigated through two-dimensional dynamic analysis. The models with geocells arranged as fascia are found to provide uniform confinement along the entire elevation whereas the reinforcement model forms a better integration of reinforcement with backfill thereby improving the stability of the system.

Keywords: Slope stabilization; Geocells; Fascia; Reinforcement; Shake table testing; Numerical simulation

1 INTRODUCTION

Geosynthetics, in their simplest form, are primarily used as reinforcement materials. Their applications extend to separation and drainage functions as well. In retaining structures and abutments, planar geosynthetics are often incorporated into the backfill to impart tensile strength to the soil, thereby achieving mechanical stabilization. Traditionally, rigid facings such as panels, segmented blocks, or gabions are employed to retain the soil. However, these facing units present challenges during construction due to their heavy weight, handling difficulties, and manufacturing complexities.

Geocells, a type of three-dimensional, honeycomb-shaped geosynthetics made from high-density polyethylene (HDPE) sheets, offer a versatile alternative. These sheets are ultrasonically welded together to form cellular structures, which are then filled with granular soil to create an effective soil-geocell wall interface. The unique three-dimensional structure of geocells provides an additional confinement effect (Bathurst and Rajagopal, 1993) not only for the infill soil but also for the surrounding soil layers. This confinement effect enhances the geocells' ability to function as both a reinforcing and a facing component. When stacked vertically, geocell layers serve as an efficient facing system, comparable to a gravity retaining wall, especially when the layers are wider at the toe and taper towards the crest (Leshchinsky et al., 2009). The advantages of geocells include ease of transportation in collapsed bundles, lightweight construction, and faster installation, making them a practical alternative to traditional rigid facings.

For structures like slopes which are not supported on its face, the additional confinement provided by geocells significantly contributes to stabilization, especially under seismic shaking. When subjected to such loading scenarios, stress reversal is inevitable. Understanding how geocells function as both reinforcement and facing under sinusoidal or seismic shaking is crucial for informed design decisions. Therefore, it is essential to investigate the behavioral characteristics of geocell layers and how their performance varies based on their application as reinforcement or facing.

Motivated by these considerations, slope models were constructed with geocell layers introduced into the backfill as reinforcement and as a supporting structure to the slope face in the form of fascia. Shake table tests were conducted to

compare their behavior under sinusoidal and seismic loading. Numerical simulations employing finite element analyses were then performed to explore the nuances of their behavior during stress reversals when implemented as reinforcement and fascia in slope stabilization.

2 MODEL DESCRIPTION

This study includes the interpretations from experimental observations and its numerical investigations. The corresponding model descriptions are given below

2.1 Lab-scale experimental model

The slope models with reinforcements and retaining components are constructed in a rigid Perspex tank to a height of 600 mm with a slope face inclination of 40° and 60° where geocells are introduced as reinforcement (R) and fascia (F) respectively. Two reinforcement layers are utilized in R model and are located at the same level as the 2nd and 4th fascia units from the toe to make a better analogy in behavior. Styrofoam sheet of 500 mm thickness is fixed to the rear wall of the tank to reduce wave reflections. Geocells made of high-density polyethylene (HDPE) of size 330 x 100 mm, are cut to fit the 575 mm width of the tank. The slope is constructed using cohesionless soil with peak friction angle of 46.8°. The infill material for geocell is the same as the backfill. Fig. 1(a) and 1(b) displays the layout of the experimental setup adopted along with the instrumentations utilized to study the seismic responses of the model. These models are subjected to horizontal motions of 1995 IndoBurma EQ (IB) and 1994 Northridge EQ (NR) with PGA of 0.08g and 0.56g respectively. The corresponding ground motion parameters are listed in the Table 1. The Fourier spectra of the same is given in the Fig. 2.

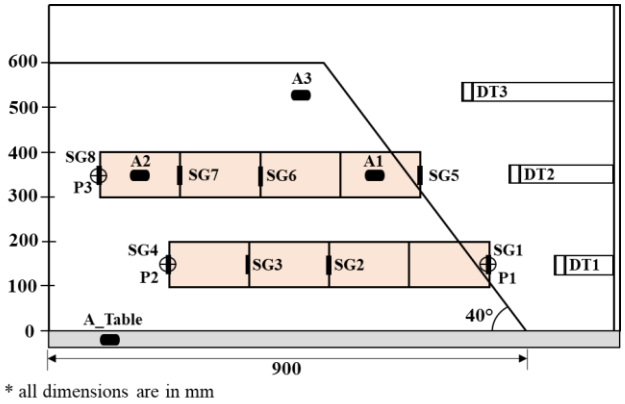

Fig. 1(a). Experimental setup with geocells as reinforcements

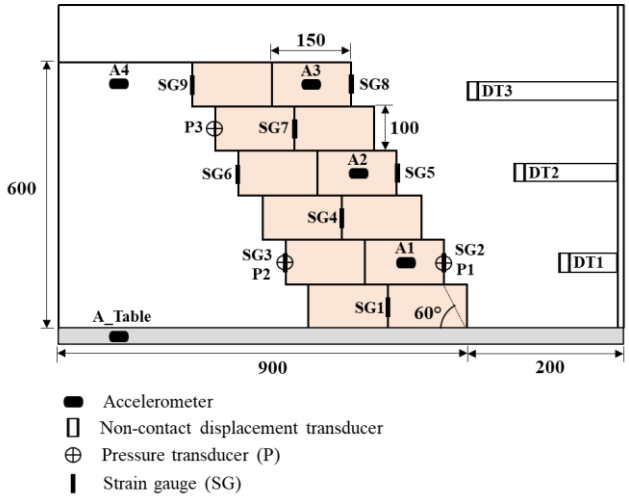

Fig. 1(b). Experimental setup with geocells as fascia elements

Table 1. Ground motion parameters for the motions adopted in this study.

Parameters	1995 IndoBurma EQ	1994 Northridge EQ
PGA (g)	0.08	0.56
PGD (cm)	0.68	9.03
RMSA (g)	0.012	0.067
Arias Intensity, I_a (m/s)	0.12	2.73

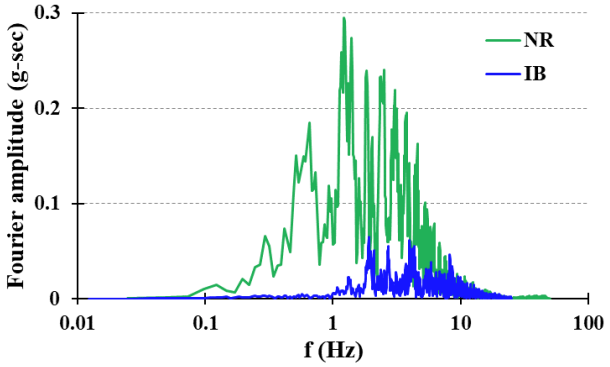

Fig. 2. Fourier spectra of IndoBurma (IB) and Northridge (NR) earthquake motions

2.2 Numerical model

Through experimental investigations, the responses can only be studied at the instrumented locations. To overcome this limitation, the lab-scale model constructed on the shake table is replicated numerically in a 2D plane-strain domain with geocells being modelled as an equivalent composite material as illustrated by Sureka *et al*. (2024). The mesh element size falls under the criteria for wave propagation problems as given by Kuhlemeyer and Lysmer (1973). The base is assumed to be fixed while the lateral boundary is retrained against horizontal movement but free from settling vertically.

3 EXPERIMENTAL RESULTS

The input command to the shake table is given in the form of displacement time history. Hence, the corresponding displacement inputs of IndoBurma EQ (0.08g) and Northridge EQ (0.56g) are used to study the response of the F and R models. A force balance accelerometer is fixed on the shake table to measure the acceleration input that is fed to the models constructed. Figure 2 shows the acceleration time histories of IB motion recorded at the table level. Even though the input displacement time history fed to the shake table is the same for both cases of F and R, the table responses recorded are not identical at the pre-peak portion of the seismic wave, which is attributed to the operational issues in the shake table that contributes to unwarranted noise to the original input motions. This observation is well pronounced in case of IB motion due to its lesser magnitude. The piston movement governing the movement of shake table depends on the high-pressure oil pumped to the actuator whose pressure magnitude is further governed by the magnitude of the command displacement given. Hence, the observational differences can be due to the payload differences that governs the ability of the actuator to pump the oil in and out of the system or external mechanical interactions during the test. Furthermore, the PGA of the input motions is not the same as the motion used as input command. The recorded responses show PGA of 0.1 g and 0.8 g for IB and NR motions respectively (Figs. 2 and 3). The same has been used in studying the responses of the models. This recorded data of table acceleration response will be considered as the input or base acceleration to study the model responses in the upcoming sections.

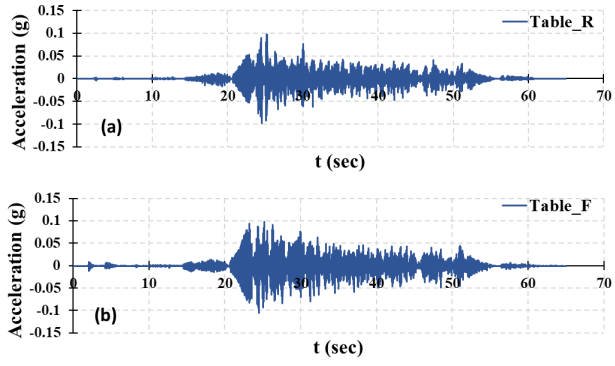

Fig. 2. Table acceleration response for IB motion with respect to (a) R and (b) F models

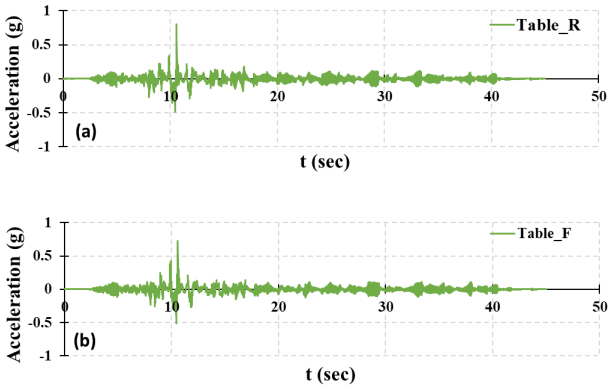

Fig. 3. Table acceleration response for NR motion with respect to (a) R and (b) F models

The slope face inclination of the fascia model is 60°. Similar slope inclination could not be achieved in case of R model since there was no fascia geocell pockets available to retain the backfill soil in between the reinforcements. The slope face inclination achieved through only geocell reinforcement is around 40°. Due to the difference in the geometry of the structure, the payload difference had come about between F and R which has contributed to the difference in the table response at the beginning of the input motion leaving the peak instances unaffected. The ground motion characteristics of the table response is studied for any major change in the energy imparted to the model which was proved otherwise since there was no significant difference observed.

3.1 Acceleration response

The acceleration response recorded in the slope face (using the accelerometers A) is utilized to calculate the amplification in the acceleration for R and F model as shown in Fig. 4. The IB motion with lesser PGA has amplified along the slope elevation. The amplification is about twice the base acceleration for R model and 1.5 times the base acceleration in F model. Geocells as fascia has yielded lesser amplification due to its confinement effect and increase in stiffness. R model, being relatively less stiff, has exhibited higher amplification. The higher PGA motion has induced deamplification in the acceleration response. Further, geocells as only reinforcement has deamplified to a higher extent than fascia.

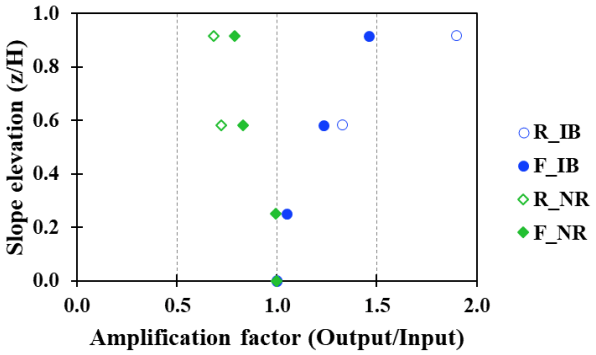

Fig. 4. Amplification of acceleration responses in fascia and reinforcement models

3.2 Displacement of slope face

Three non-contact displacement transducers (DT) were installed through an external post to measure the lateral displacement of the face. They were located near the toe, mid-height and crest. The level of measurement of the displacement transducers remains the same for both R and F. The top-most displacement transducer (DT3) near the crest, points to the geocell fascia in case of F model and the sand slope face in case of R model.

The displacement magnitude noted under IB motion is very negligible and, hence, it is not included in this paper. The displacement response pertaining only to the NR motion is discussed. In R model, displacement at the crest is mainly due to the dislodging of soil mass. Due to its cohesionless nature, the sand particles roll down the crest during the seismic loading and settle near the mid-slope or the toe. This caused the inward movement of the slope face at the crest which is very evident in the time history recorded (Fig. 5). The displacement of crest in the positive axis portrays the crest caving in under NR seismic event.

The presence of geocell reinforcement was found to control the displacement of the slope face until a certain extent, in comparison to the response of the sand slope. However, the overall peak displacement recorded during the seismic loading is greater in case of R due to nil confinement at the slope face. In case of fascia (Fig. 6), the lateral displacement is significantly restricted by the confinement effect provided by the geocell pockets. It should be noted that the interlayer friction between the geocell layers played a vital role in controlling the sliding of the individual geocell layers. The topmost reinforcement layer in R model is sandwiched between the sand layers. Hence, due to the absence of the interlayer friction between geocell layers in combination with the confinement effect provided by the same, the reinforcement layer at the mid-height displaced to a higher magnitude. This occurrence is highly obvious just around the peak event where the peak displacement magnitude is noted to be around 34 mm. Furthermore, the bottom reinforcement layer displaces relatively lesser due to lesser acceleration amplification at its level and relatively higher overburden pressure than the upper reinforcement layer. The residual displacement noted in the response time histories show that even if the structure undergoes a significant displacement magnitude under a seismic event, geocell layers help in retrieving it back leaving a minor residual displacement. The absence of the same caused the crest to cave in.

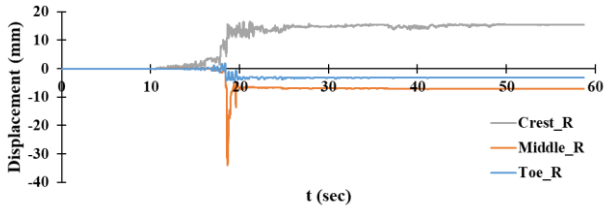

Fig. 5. Lateral displacement of slope face in R model under NR motion

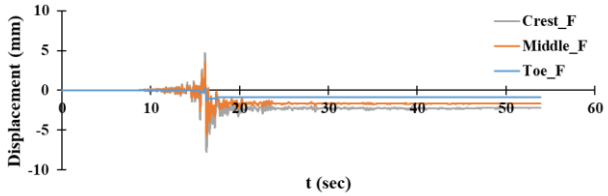

Fig. 6. Lateral displacement of slope face in F model under NR motion

3.3 Tensile strain in geocells

Linear strain gauges (SG) are glued to the geocell walls in the locations shown in the Fig. 1 to determine the tensile strain developed in the geocell walls under seismic loading. The data is recorded in micro-strain (μm/m) and then converted to strain percentage. The strain recorded under IB motion is very less relative to the ones recorded under NR motion due to the difference in their magnitudes. Hence, under IB motion, only the frontal geocell walls of R model, which holds the infill on one side and has a free surface on the other, were in tension (Fig. 7). No strain was recorded on the geocell pockets along further length of geocell layer inside the backfill.

The tensile strain recorded in the frontal face of geocell walls in R model under IB motion is shown

in Fig. 7. It can be noted that the tension in the top reinforcement is greater than that of the lower one. However, no such strain was observed in the geocell walls of F model positioned at the similar elevation as geocell reinforcement. The tensile strain recorded at the crest is the only significant one noted under the same motion. This strain is contributed by the topmost layer of backfill. The magnitude of strain at the crest of fascia is found to be higher than that developed in the frontal face of reinforcement. In fascia, the deformation is restrained throughout the slope height by the geocells and when the confinement decreases towards the crest, displacement increases thereby causing the strain in the geocell walls to increase. Such confining effect is absent in only reinforcement case, allowing the structure to deform, thereby inducing lesser strain in geocells.

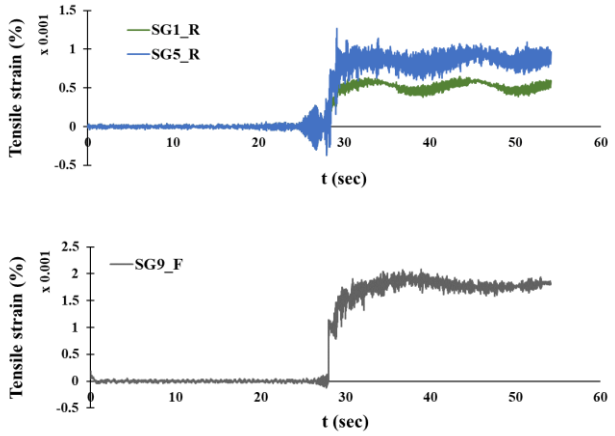

Fig. 7. Tensile strain in (a) R and (b) F model under IB motion

Under a high magnitude EQ motion (0.8g), all the geocell pockets of the reinforcement comes into action. Fig. 8 shows the tensile strain developed in the bottom layer of reinforcement under NR motion. It can be seen that the strain decreases from the frontal face till the rear end buried inside the backfill. The same trend can be witnessed in the fascia pockets as well. However, the tensile strain developed in the geocell walls near face of the reinforcement layer exhibits a higher strain magnitude than that of the fascia pockets which also occupy the same position as that of the reinforcement layer. This is because the bottom reinforcement is sandwiched between sand layers and the strain developed in the same is affected from supporting the upper sand layer as well. In case of F model, it is taken care by the successive geocell fascia pockets as the strain is distributed between them instead of getting it concentrated in one layer.

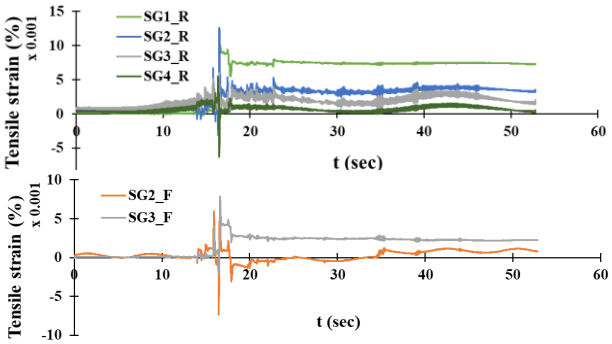

Fig. 8. Tensile strain developed in the bottom geocell reinforcement layer and its corresponding fascia pockets under NR motion

The tension developed in the geocell walls of the top reinforcement layer is then assessed in comparison with the ones developed in the fascia geocells located at the same elevation in the F model. It can be noted that unlike the bottom reinforcement where all the geocell walls were under tension, only the frontal face of the geocell reinforcement is under tension while the ones further inside the backfill are under compression. This shows that the geocells at the rear end are pushed outward to a certain extent causing compressive strain. It can also be related to the higher displacement magnitude recorded at the frontal face of the same layer. The magnitude of compressive strain is greater than or equal to the tensile strain developed at the frontal wall. When one of the two geocell walls forming a pocket is moved apart in expansion, tension occurs and when it is moved towards the other, compression is noticed. In case of fascia as well, the geocell wall at the frontal end is under tension and the rear end is relatively under compressive strain. However, the higher magnitude of the residual tensile strain than the fascia beneath also supports the relatively higher displacement recorded at the mid-height than toe.

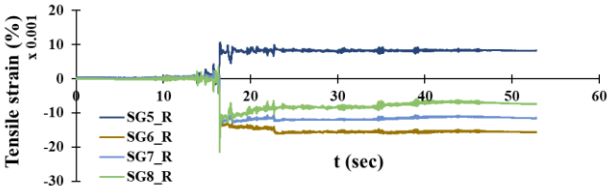

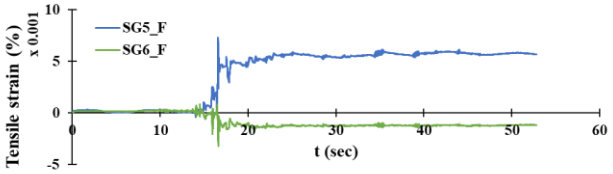

Fig. 9. Tensile strain developed in the top geocell reinforcement layer and its corresponding fascia pockets under NR motion

3.4 Lateral stress

Pressure transducers (P) are attached to the geocell walls as shown in Fig. 1 to quantify the lateral stress exerted by the backfill and the infill material on the geocell walls. For this purpose, two transducers have been attached to the rear walls and one to the frontal wall. The data recorded contains a little bit of noise in case of lower magnitude motion (Fig. 10). Filtering was adopted to the extent that the peak magnitude of the data recorded is unaltered.

Assessment of lateral stresses exerted at P1 gives the stresses exerted by the infill material on the frontal geocell wall. The lateral stresses exerted under IB motion is shown in Fig. 10. In case of R model, the stress magnitude is more due to the lesser confinement along the slope face. At P2, both R and F model experienced negligible lateral stresses, hence neglected here. At P3, the lateral stress exhibited in the reinforcement model is higher indicating higher lateral stresses induced by the backfill to the geocell layer. This can also be due to the boundary effect in the model as the tank boundary was closer to the end of the reinforcement while it was otherwise in case of fascia.

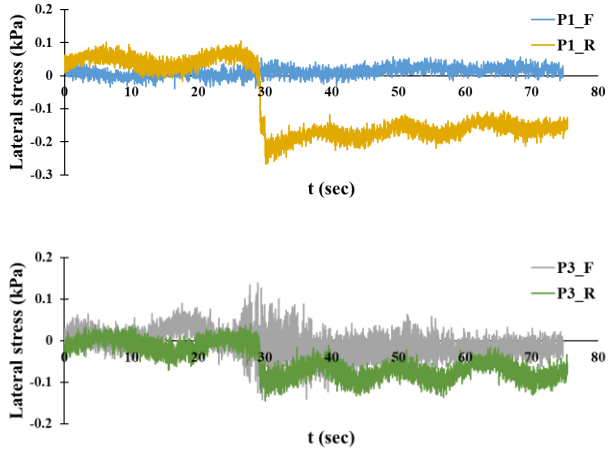

Fig. 10. Lateral stresses exerted under IB motion

In case of higher magnitude seismic wave input, the peak values of lateral stress exerted can be clearly observed from the response time history. The lateral stress recorded at P1 by the infill soil is higher in fascia due to the higher overburden caused by the upper fascia layers. This effect is considerably lesser in case of reinforcement due to gentler slope inclination which induces lesser overburden pressure.

Under a high magnitude motion (Fig. 11), the lateral stress exerted at P3 in the top reinforcement layer gives a sharp peak due to the compressive action of the interior geocells as explained in the previous section. The difference in peak magnitude exerted at P2 and P1 in R and F model explains the function of reinforcement and fascia. In case of fascia, P2 is less than P1 as the fascia is sandwiched between fascia elements giving higher overburden pressure. It denotes that the stress exerted at the face by the infill is higher than the ones exerted by the backfill on the rear face. Likewise, the strain exerted at the frontal face is also higher than the rear face. In case of reinforcement, the stress exerted at the rear face (P2) is higher than that is exerted at the front face (P1); whereas, the strain exerted at rear end of the geocell layer is very less when compared to the frontal face. Increased stress and strain at the front face indicates a localized deformation that can cause the face to bulge or slide outward. The reinforcement model shows a better integration of the reinforcement with the backfill through the increased stress recorded at the rear end, thereby improving the stability of the system.

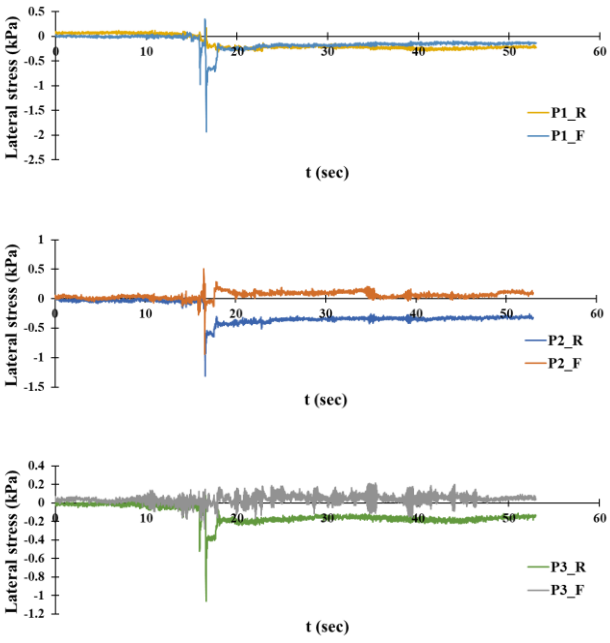

Fig. 11. Lateral stresses exerted under NR motion

4 NUMERICAL ANALYSES

Fascia and reinforcement models constructed on the shake table is replicated numerically with the same slope face elevation of 60˚. Three monitoring points are located close to the slope face and three on the backfill to study the hysteresis response of the lab-scale model. The hysteresis curves plotted at the response of these monitoring points exhibit a linear behaviour under the given motions. This can be due to the apparent increase in the stiffness of the system after scaling down or the original motion utilized to study the seismic responses not being strong enough to induce non-linearity in the model.

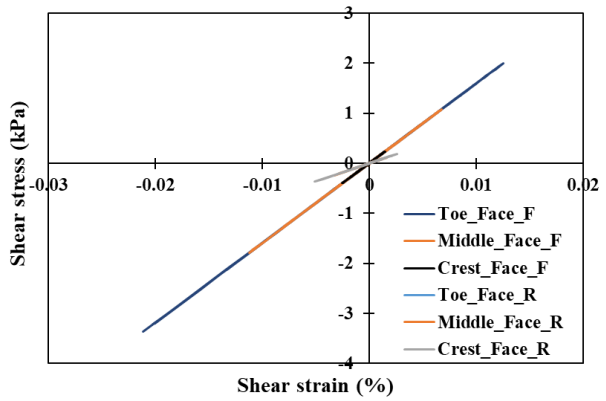

Fig. 12. Hysteresis response of the slope face under NR motion

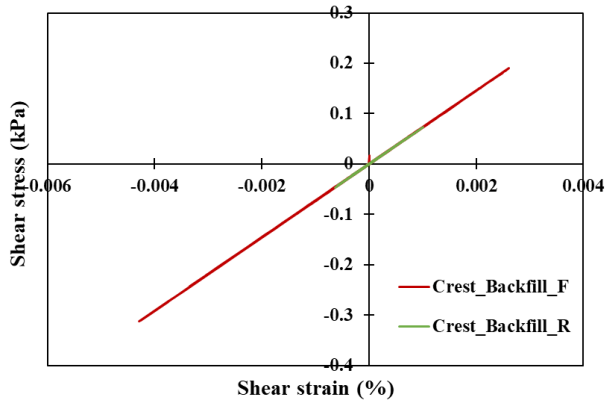

Fig. 13. Hysteresis response of the backfill under NR motion.

Due to the presence of fascia all along the elevation of the slope face, the gradient of the hysteresis curves is steeper than the R model (Fig. 12). This indicates the increase in shear stiffness of the slope face due to the introduction of fascia. Geocells, as fascia, acts as a stress attractor thereby exhibiting higher shear stress magnitude. Likewise, the slope with reinforcement exhibits lesser shear range during the seismic event.

The hysteresis behaviour of the backfill (Fig. 13) is studied for geocells as reinforcement and fascia. The increment in the confining pressure induced by the fascia geocells increased the shear stiffness of the backfill giving rise to a broader shear range. Although the geocells are introduced as reinforcements in the slope, it did not provide the confining effects sufficient enough to increase the shear stiffness of the backfill.

5 CONCLUSIONS

Based on the conducted experimental studies and numerical assessments, the following conclusions can be drawn:

- Introducing geocell layers only as reinforcements does not provide uniform confinement throughout the slope elevation leaving the unconfined part vulnerable to cave in. However, geocell pockets as fascia gives better confinement and retains the backfill effectively resulting in lesser displacement.

- Geocell reinforcement layers tend to move outwards in the absence of any locking interlayer friction above and beneath it. The presence of such locking interfaces in facia helps to control such sliding of individual layers effectively.

- Development of strain concentration is noticed when geocells are introduced as just reinforcements. Instead, introducing geocells as fascia helped in distributing the strain to the successive geocell layers all along the elevation. Geocell pockets towards the front of the slope experienced higher tension which decreased along the interior geocell pockets.

- Introducing geocells only as fascia or as reinforcements holds its own advantages and disadvantages. However, implementing geocells as fascia and reinforcement can nullify the cons and make the system function effectively even under dynamic loading conditions.

ACKNOWLEDGEMENTS

The authors would like to express sincere gratitude to Strata Geosystems Pvt. Ltd. for providing the necessary geocells to conduct this research work.

REFERENCES

Bathurst, R. J., & Rajagopal, K. (1993). Large-Scale Triaxial Compression Testing of Geocell-Reinforced Granular

Soils. Geotechnical testing journal, 296-303.
Kuhlemeyer, R. L., & Lysmer, J. (1973). Finite element method accuracy for wave propagation problems. Journal of the Soil Mechanics and Foundations Division, 99(5), 421 427.
Leshchinsky, D., Ling, H. I., Wang, J. P., Rosen, A., & Mohri, Y. (2009). Equivalent seismic coefficient in geocell retention systems. Geotextiles Geomembranes, 27(1), 9-18.
Sureka, S., Wable, A., Lhousa, V., Lupheng, C. and Dey, A. (2024) Stability and seismic response analysis of geocell reinforced slopes based on an equivalent composite approach. *Japanese Geotechnical Society Special Publication*: 10(25), 930-93